Exploring the Solvation of Acetic Acid in Water Using Liquid Jet X-ray Photoelectron Spectroscopy and Core Level Electron Binding Energy Calculations

*Jared P. Bruce[†], Kimberly Zhang, Sree Ganesh Balasubramani, Amanda R. Haines, Randima P. Galhenage, Vamsee K. Voora[††], Filipp Furche, and John C. Hemminger**

Department of Chemistry, University of California, Irvine, Irvine, California, USA 92697

Email: jchemmin@uci.edu

Current Addresses:

[†]Department of Interface Science, Fritz Haber Institute, Berlin, Germany 14195

[††] Department of Chemical Sciences, Tata Institute of Fundamental Research, Homi Bhabha Road, Colaba, Mumbai 400005

Abstract

Liquid jet X-ray photoelectron spectroscopy was used to investigate changes in the local electronic structure of acetic acid in the bulk of aqueous solutions induced by solvation effects. These effects manifest themselves as shifts in the difference in the carbon 1s binding energy (ΔBE) between the methyl and carboxyl carbons of acetic acid. Furthermore, molecular dynamics simulations, coupled with correlated electronic structure calculations of the first solvation sphere, provide insight into the number of water molecules directly interacting with the carboxyl group that are required to match the ΔBE from the photoelectron spectroscopy experiments. This comparison shows that a single water molecule in the first solvation shell describes the photoelectron ΔBE of acetic acid while upwards of 20 water molecules are required for the conjugate base, acetate, in aqueous solutions.

Introduction

A variety of spectroscopic techniques have been used to probe the changes in the electronic structure of solute molecules resulting from solute/solvent interactions.[1,2] Nuclear magnetic resonance (NMR) spectroscopy has been utilized to study transition metals in solution,[3] while infrared (IR) and UV-vis spectroscopy have been used for organic species in different solvents.[4–6] In general, these experiments are sensitive to the valence electronic structure of the solute, thus providing information on the solute/solvent interaction that is somewhat delocalized due to the spatial extent of the valence orbitals. By probing core level electrons, X-ray absorption (XAS) and emission (XES) spectroscopies provide information on the electronic structure that is more localized in the region of the ionized atom and have been used to investigate shifts in the electronic structure at different mole fractions.[7–9] From a theoretical standpoint, electronic structure calculations, coupled with molecular dynamics (MD) simulations, can offer significant insight but require high quality structural information from diffraction studies, in addition to the spectroscopic work, to verify the accuracy of the simulation.[10]

Acetic acid is a widely used, industrially relevant molecule that is one of the simplest carboxylic acids having several points of possible interaction with a solvent through hydrogen bonding.[11] In the gas phase, the accepted structure is a cyclic dimer that has been shown by molecular dynamics (MD) simulations and diffraction experiments.[12] Acetic acid in the liquid phase presents a different challenge regarding the solvation and hydrogen bonding network associated with the molecule in solution from both an experimental and theoretical point of view.

There are few techniques that can be used to directly investigate the local electronic structure within a molecule **in solution**. By probing core level electrons, X-ray photoelectron spectroscopy (XPS) provides information about the local electronic structure within the molecule. Recent

advances in instrumentation, including electron transfer lenses and differential pumping, have enabled characterization of liquid/vacuum and liquid/gas interfaces using liquid jet ambient pressure XPS (LJ-APXPS).[13–16] XPS has been shown to be sensitive to changes in the local chemical environment of aqueous solutions, such as changes in concentration and pH,[17,18] and could be used to understand the solvation of a molecule such as acetic acid by investigating the relative change in chemical environment between the carboxyl and methyl carbons in the molecule. In aqueous solution, this would provide additional understanding of the solvation of acetic acid and can also be used to investigate changes in solvation when other solvents are used.

Here, we make use of the recently developed self-consistent generalized Kohn-Sham semicanonical projected random phase approximation (GKS-spRPA) method to compute core electron binding energies (CEBEs).[10] GKS-spRPA has been shown to yield CEBEs with an accuracy comparable to that of high-level propagator theory but significantly lower computational cost, enabling applications to solvated species with high predictivity. The comparatively low-cost of GKS-spRPA enables the computation of the CEBEs in conjunction with the *ab initio* trajectories obtained from hybrid or semilocal density functional approximations. This combined approach can be used for systematic study of microsolvation effects. It is well established that valence[19] and core[20] ionization potentials converge very slowly with the number of solvent molecules surrounding the solute. Here, we used a combination of continuum solvation models and *ab initio* MD (AIMD) to speed up the convergence of the CEBEs.

In the work described here we have used lab based LJ-APXPS experiments coupled with detailed calculations of the core level binding energies of acetic acid and acetate in aqueous solutions. These experiments utilize Al Kα (1486 eV) X-rays resulting in high kinetic energy photoelectrons that probe the behavior in the bulk of the solution. We follow the difference in

binding energies of the C1s electrons for the methyl and carboxyl carbons as a measure of the impact of solvent interactions on the local electronic structure within the molecule. By comparing measured and calculated core level binding energies we find that the majority of the solvent induced change in the electronic structure probed in the XPS experiment is due to the interaction of one water molecule with the hydroxyl group of acetic acid. In stark contrast we find that 20 water molecules are required in the case of the acetate ion.

Methods

Liquid Jet X-ray Photoelectron Spectroscopy

Solutions were prepared at a 5 M bulk concentration in water. A small amount of NaCl (0.02 M) was added to the solutions to prevent charging of the liquid jet. Acetic acid and sodium acetate (Sigma Aldrich, ACS Reagent) were all used as received without any purification. The solutions were then characterized immediately after mixing with no modifications in pH (~2.0 in the acetic acid case and ~9.5 in the case of the acetate solutions). Photoelectron spectra were collected on a lab-based, near ambient pressure X-ray photoelectron spectrometer from SPECS Surface Nano Analysis Gmbh specifically designed for liquid jet experiments. Monochromatic Al Kα (1486 eV) X-rays with a 40 μm diameter spot size was used in these studies. At this excitation energy, the generated C1s photoelectrons are produced with a kinetic energy of ~1200 eV. At this kinetic energy the electron escape depth from the solution is ~5 nm.[21] Our previous synchrotron based experiments on a variety of small molecular solvents in water have shown that spectra obtained at this high photoelectron kinetic energy are characteristic of the **bulk** solvation of the molecule.[14,22–25] All liquid-phase photoelectron experiments followed similar procedures to earlier work completed at synchrotron facilities outlined in detail elsewhere.[23,24,26,27] The pressure in the liquid jet chamber was held at ~8 mbar by the use of a cooled (~5 °C) bath of NaCl saturated water which

also acted as the collector for the liquid jet as it exits the chamber. Gas phase spectra are obtained with the liquid jet positioned away from the entrance to the electron analyzer, ensuring no liquid phase peaks appear. Liquid phase spectra are collected with the liquid jet near the analyzer cone and contain both gas and liquid phase spectra. All liquid spectra are collected after the liquid jet has been moved into the appropriate position approximately 25μm from the analyzer cone entrance (300 μm diameter). The liquid jet is operated at a flow rate of 0.4 mL/min.

All liquid jet XPS spectra were collected at 50 eV analyzer pass energy and were calibrated to the O 1s gas phase of water at 535.5 eV. Since small charging effects can occur that may impact the absolute binding energies, this study focused on the differences in binding energy between the carboxyl and methyl carbon (ΔBE) to compare with theoretical calculations. The energy resolution of the analyzer at this pass energy is 1.0 eV.

Electronic Structure Calculations

Total energy calculations were performed on several potential starting structures for each system; the structure with the minimum total energy of each system was used as the starting structure for the following steps. The geometry optimization was performed within density functional theory (DFT) using the PBE0 functional and the def2-SVP basis set.[28,29] Grid size 3 was used for numerical integration, and self-consistent field (SCF) convergence criterion of 10^{-8} was used.[30] Numerical finite differences of gradients (NumForce program in TURBOMOLE) were used to confirm that the geometries obtained reside at local minimum energy.[31] To simulate acetic acid and acetate in liquid phase, a small number of explicit water molecules were included. Calculations for molecules in dielectric medium were also performed employing the conductor-like screening model (COSMO) with the dielectric constant for water, 80.1.[32,33]

Ab Initio Molecular Dynamics Simulations

To simulate the chemical systems studied in the experiment more accurately, a trajectory of structures, instead of a single point structure, was investigated for each system. Microcanonical ensemble *ab initio* molecular dynamics (AIMD) including n=1-6 number of water molecules was used.[34] The AIMD simulations were run for a total of 10 picoseconds (ps) with 20 a.u. (0.5 fs) time steps; the PBE0 functional and def2-SVP basis sets were employed. The starting temperature of the AIMD simulation was 500 K. The first 4 ps of the trajectories were discarded to allow equilibration, and 50 representative snapshots were extracted randomly from the next 6 ps of the trajectory. We extracted 500 snapshots from each trajectory initially; in an attempt to obtain a more efficient sampling by reducing the number of snapshots, we extracted 50 samples from the 500 snapshots and performed bootstrapping analysis. The 95% confidence interval calculated with these 50 snapshots was within 0.002 eV of the sample average. This indicates that these 50 snapshots provided an equilibrium ensemble which reasonably represented the clusters that existed in the liquid jet experiment.

Core Electron Binding Energy (CEBE) Calculations

The structures of the 50 equilibrium snapshots from the AIMD trajectories were extracted to set up the CEBE calculations using the GKS-spRPA method. For these calculations, 400 imaginary frequency integration points,[10] the PBE exchange-correlation potential along with the def2-TZVPP basis set,[29] grid size 4 for numerical DFT integration and SCF convergence criterion of 10^{-8} were used. The CEBE of the different systems with various numbers of water molecules were reported as the average of the representative 50 snapshots. The starting geometries of the acetic acid and acetate systems were built using Avagadro.[35] All calculations were performed using the TURBOMOLE V7-4 program package.[36]

Solvation Effects

We included COSMO to account for implicit solvation to simulate liquid phase acetic acid and acetate. The current implementation of the GKS-spRPA includes continuum solvation effects on the KS reference and partially on the correlation energy. However, even a full GKS-spRPA COSMO implementation, which is currently not available to us, may not capture additional effects caused by inner-shell solvation.[37] Additionally, the COSMO solvation model has been parameterized using solvation free energies, which does not necessarily imply accuracy for CEBEs.

Results and Discussion

An understanding of the electronic structure in gas phase is needed to compare with the molecule in solution and, eventually, with theory. Figure 1 shows the C 1s gas and liquid spectra of the aqueous acetic acid and the C 1s spectra for aqueous sodium acetate obtained from LJ-APXPS experiments. Note that, as expected, there is no gas phase component for the acetate.

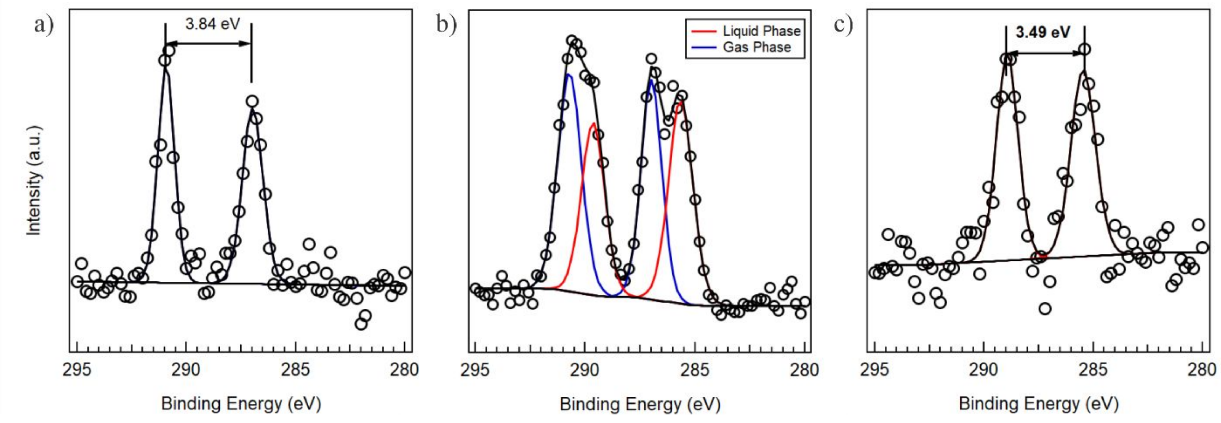

Figure 1: C 1s LJ-APXPS spectra of (a) gas phase acetic acid above the liquid jet, (b) 5 M aqueous acetic acid showing both the gas phase acetic acid and the acetic acid dissolved in the solution and (c) 5 M aqueous sodium acetate solution (pH ~ 9.5). The opposites slopes are a fitting artifact from the large scatter of the background data points due to the low signal values. The choice of endpoints for the fitting of each spectrum were the same value with an average of 10 points on either side. The ratio of the peak areas resulting from the fit was 1:1 in all cases.

As can be seen in Figure 1, the C 1s peaks due to the methyl (285.6 eV) and carboxyl (290.9 eV) carbons are easily separated in the spectra. The difference between the two peaks in the C 1s spectrum (ΔBE) can be used to show any perturbation of the electronic structure of the molecule in relation to its solvation. A Monte Carlo simulation of the peak model was used to estimate the errors in the peak position and full width at half maximum (FWHM).[38] A summary of the binding energies, ΔBE values, and the peak FWHM values for all the relevant peaks is provided in Table 1.

Table 1: Summary of C 1s gas and liquid phase data of acetic acid and acetate in aqueous solution. ΔE values are the difference between the methyl and carboxyl binding energies in electron volts.*

	Carboxyl Carbon		**Methyl Carbon**		**ΔE_{gas} (eV)**	**ΔE_{liq} (eV)**
	E_b (eV)	*FWHM (eV)*	*E_b (eV)*	*FWHM (eV)*		
Acetic Acid *(gas)*	291.00 ± 0.03	0.85 ± 0.10	287.16 ± 0.05	1.22 ± 0.15	3.84 ± 0.06	-
Acetic Acid *(Liquid)*	289.66 ± 0.09	1.10 ± 0.15	285.64 ± 0.07	1.07 ± 0.16	3.90 ± 0.11	4.02 ± 0.11
Sodium Acetate	288.95 ± 0.04	1.16 ± 0.10	285.46 ± 0.05	1.31 ± 0.12	-	3.49 ± 0.06

**The errors reported in Table 1 are statistical errors. As mentioned in the Methods section there may be small systematic errors in the absolute binding energies due to minor charging of the liquid jet, which does not impact the differences in binding energies (ΔBE). We provide the measured absolute binding energies here to show the different changes in the carboxyl carbon atom BE and the methyl carbon atom BE (e.g. In comparing aqueous protonated acetic acid to aqueous acetate the change in the BE value of the carboxyl carbon is larger than that for the methyl carbon as would be expected). Such qualitative observations that rely on the absolute binding energies will not be impacted by the small systematic errors resulting from the possible small amount of charging of the liquid jet.*

The ΔBE values of acetic acid of the gas phase molecule above the liquid jet and in the liquid phase is 3.90 and 4.02 eV, respectively. The liquid phase ΔBE is increased compared to the gas phase due to the interactions with the water solvent. Acetate, the conjugate base of acetic acid, has a negative charge on the carboxyl carbon and is expected to have a different solvation in comparison to acetic acid in aqueous solution. The ΔBE for acetate in water solution is 3.49 eV. The binding energy of the acetate carboxyl carbon (288.95 eV) is lower than the carboxyl carbon

of the acetic acid (289.64 eV). The methyl group also shows a small shift of 0.18 eV to lower binding energy, consistent with an indirect effect of the deprotonation of the carboxyl group.

Electronic structure calculations using MD simulation snapshots of acetic acid and acetate anions with water solvent, as described in the Methods section, were carried out with different numbers of explicit solvent molecules using the methods described by Voora et al.[10] Electronic structure calculations were used in each configuration of the MD simulation to generate a difference in the binding energy between the carboxyl and methyl carbons (ΔBE). A summary of the ΔBE results of this method is shown below in Table 2.

Table 2: Comparison of experimental data and calculated ΔBE for acetic acid and acetate in water. The calculated ΔBE is from the averaged AIMD trajectories obtained from GKS-spRPA calculations. Higher number solvent values for acetate were calculated with point calculations and have no error in the calculated values. Experiment gas phase values are found from the fit of the liquid photoelectron spectra.

Number of Solvent Molecules	Acetic acid ΔBE in Water	Acetate ΔBE in Water
Gas Phase	3.58	-
1	3.76 ± 0.17	3.03± 0.12
2	3.82 ± 0.16	3.06 ± 0.15
3	3.77 ± 0.16	3.13 ± 0.11
4	3.82 ± 0.18	3.14 ± 0.13
8	-	3.32
10	-	3.40
20	-	3.45
Experiment Liquid	***4.02 ± 0.11***	***3.49 ± 0.06***
Experiment Gas	***3.90 ± 0.11***	**-**

ΔBE of acetic acid in the gas phase was calculated to be 3.58 eV which is lower than the pure gas phase experimental value of 3.84 eV. The difference is likely due to vibrational excitations of the PES process leading to slightly asymmetric and broader peak with lower peak height in the experiment. This was not included in the calculations. To test this, d^4-acetic acid, where the CD_3 is expected to have weaker vibrational coupling, was also characterized in aqueous solution at the same concentration (Figure S1) and was observed to have a ΔBE of 3.67 eV. This ΔBE is much closer to the calculated value compared to hydrogenated acetic acid. Other studies have shown that in the gas phase, acetic acid dimer may be a more suitable comparison to theoretical calculations.[12,39] The dimer was found to have a ΔBE of 3.64 eV for both molecules and is an appropriate structure for gas phase calculations. The addition of one water molecule to the simulation results in a significant shift from the single molecule value of 0.18 eV to a higher ΔBE. This is in close agreement with the gas to liquid phase shift observed in the experiment (0.12 eV). Including more water molecules in the local structure for the calculation results in little additional change (Table 2). Acetic acid has 3 possible locations to hydrogen bond to any solvent molecule directly: acceptors at the carboxyl oxygen and hydroxyl oxygen and a donator at the hydroxyl hydrogen. This would, as an initial starting point, indicate that a minimum of 3 water molecules could be needed to form the first strong solvent interactions in the solvation shell around the acetic acid. From a theoretical study of acid-water clusters, Krishnakumar et al. concluded that continuum solvation models insufficiently capture acetic acid microsolvation.[40] It was suggested in previous literature that the first solvation shell of an acetic acid molecule in water is 4-5 water molecules under dilute conditions.[40,41] Based on the results of the simulations in comparison to the experiment, the number of solvent molecules required to reproduce the experimental shift in the core level electronic structure from the gas to the solution value, within error, is only 1 water

molecule. Representative snapshots of the water interaction within the MD trajectory with the acetic acid are shown below in Figure 2.

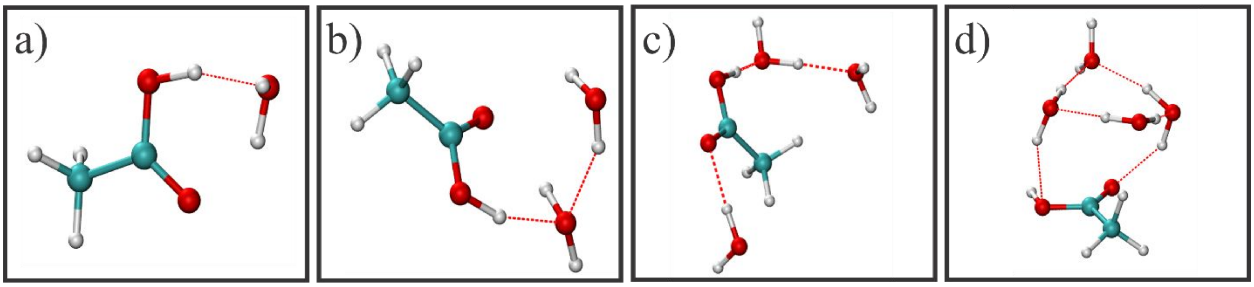

Figure 2: Representative snapshots from the MD simulations calculated at PBE0\def2-TZVPP level with (a – d) 1 to 4 water molecules, respectively.

The snapshots show the interaction of water with acetic acid begins with the hydroxyl hydrogen and the water molecule. When a second water molecule is added, there is no additional, direct interaction with acetic acid, rather, the second water molecule hydrogen bonds to the first water already bound to the acetic acid as shown in Figure 2b. This would be why the ΔBE does not shift significantly when adding a second water molecule. The addition of a third water molecule then interacts with the carboxyl oxygen of acetic acid causing a very slight decrease in the calculated ΔBE. When a fourth water is added, there is no change in the direct interaction with the acetic acid but the interaction between solvent molecules is modified and the ΔBE slightly increases again. Within the first solvent shell, there is no interaction with the methyl end of the acetic acid with the solvent molecules. Exploratory single-point calculations without COSMO showed a decrease in ΔBE by 0.2-0.3 eV indicating a slower convergence to the experimental result in the absence of continuum solvation.

Simulations and electronic structure calculations were also carried out for acetate in water, and the results are tabulated in Table 2. The ΔBE values for acetate containing up to 4 water molecules underestimates the experimental value; however, acetate is thought to contain upwards of 6 water

molecules in its first solvation shell and this could be the origin of the observed deviation.[41] This system requires more solvent molecules in the simulation to converge and to capture the experimental results, presumably due to longer range electrostatic interactions for the ionic system. A total of 8, 10 and 20 water molecules were added to the simulation and their resulting ΔBE is tabulated in Table 2.

For acetate with 10 water molecules, the simulation begins to capture the local solvation structure that would correspond to the resulting ΔBE of the photoelectron experiments. This indicates that complex interactions that occur between the analyte and the solvent will require more solvent molecules to be included in the local electronic structure calculation to reproduce experimental values. The charged nature and delocalized carboxyl group of acetate would require more solvent molecules in the calculation. Snapshots of these interactions are shown below in Figure 3.

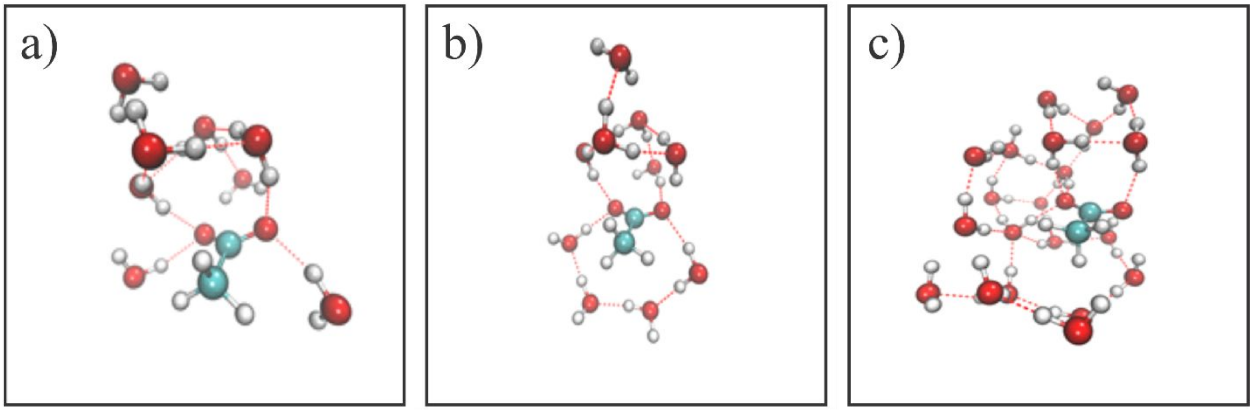

Figure 3. Optimized geometries of (a) $CH_3COO^-\cdot 8\ H_2O$, (b) $CH_3COO^-\cdot 10\ H_2O$ and (c) $CH_3COO^-\cdot 20\ H_2O$ using the PBE0 functional with def2-TZVPP basis set for all the atoms.

Similar to acetic acid, the snapshots show that all of the interactions between the solvent molecules and acetate ion are located at the carboxyl group of the molecule with almost no interactions near

the methyl group. The effect of continuum solvation was found to have an even larger effect on computed ΔBE values for acetate than for acetic acid: For acetate with a single water molecule, COSMO solvation increases ΔBE by approximately 0.7 eV. The magnitude of the COSMO contribution is found to decrease slowly as the number of water molecules increases, suggesting that the screening of long-range electrostatic interactions simulated by continuum solvation is vital for capturing the bulk solvation limit.

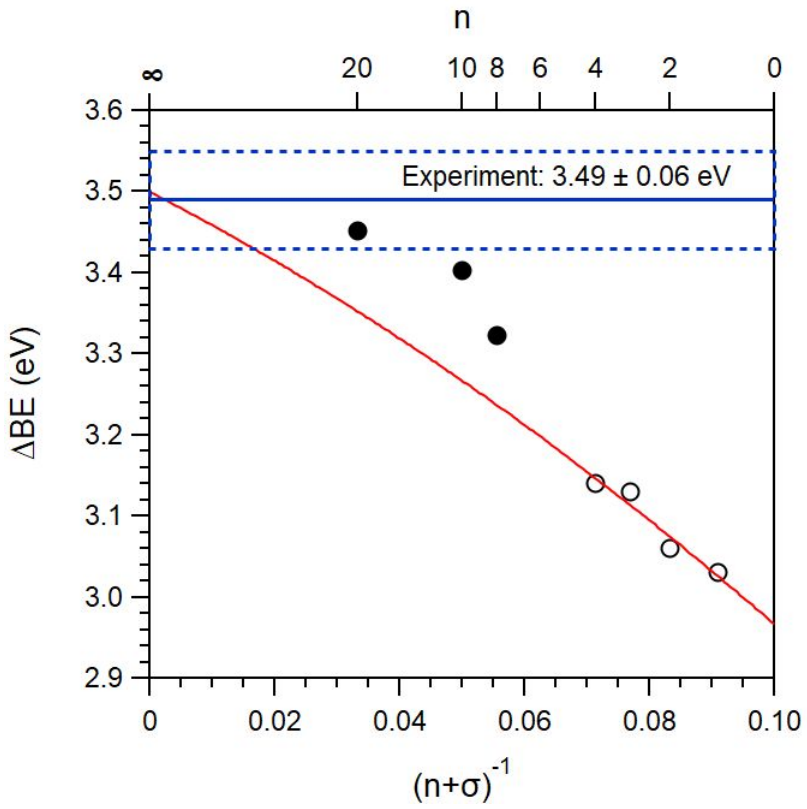

Figure 4: Difference in binding energy (ΔBE) of acetate with finite number of water molecules (n) as a function of $n + \sigma$ where $\sigma = 10$, compared with the experimental value. The unshaded points are obtained from the average ΔBE obtained from the MD trajectories, and the shaded points are obtained from single point calculations.

While the first water molecule is enough to capture almost all the solvation effects for acetic acid, it is obvious that in the case of acetate, implicit solvation and explicit solvation combined was not sufficient to simulate liquid phase acetate anions. As is indicated in Figure 4, the calculated ΔBE of acetate with 20 water molecules is 3.49 eV, which matches well with the

experimental value. To further investigate this issue, apart from explicit solvation for near field effects and continuum solvent, extrapolation was included to calculate the CEBE of solution phase acetate. When a negatively charged molecule in finite-size clusters interact with solvent molecules with unknown potentials, the extrapolation model for size-dependent binding energy can be derived based on classical polarization theory. The existing mathematical model states that the binding energies of a negatively charged solvated ion scales linearly as 1/R, where R is the radius of the solvated cluster.[42] However, this mathematical model performs poorly when applied to small clusters, and the performance is highly dependent on the type of system. The extrapolation result obtained from this model is reported to deviate significantly from the experimental result. To specifically address the issues discussed, Pathak and co-workers[43] developed a new extrapolation model in the form of a truncated Taylor series:

$$\Delta E_v(n) = \Delta E_v(\infty) + \frac{A_v}{n+\sigma} + \frac{B_v}{(n+\sigma)^2}$$

where n is the number of explicit solvent molecules, and σ is a positive integer that is greater than unity. By plotting the ΔBE obtained from the finite-sized clusters, a polynomial trend line can be obtained based on the extrapolation method described above, and the second polynomial is calculated to be $y = -13.52x^2 - 3.98x + 3.50 \; where \; R^2 = 0.9387$, where the CEBE liquid phase acetate is determined by the y-intercept of the polynomial trend line (Figure 4). The CEBEs of acetate ions from single point calculations were used to test the validity of the extrapolation model. The parameter sigma was chosen to equal 10, an order-of-magnitude estimate based on Ref. 36; however, the bulk extrapolated result was found to be fairly insensitive to sigma.

The number and distribution of solvent molecules had a much greater effect on the chemical shift of the negatively charged acetate than on neutral acetic acid. Unlike acetic acid,

where we capture bulk behavior with the addition of only one directly interacting solvent molecule, acetate demonstrated behavior that is extremely sensitive to change in solvent environment.

Conclusion

Liquid jet APXPS was used to provide insight into the solvation environment of small molecules by investigating the change in electronic structure of acetic acid and acetate in aqueous solutions. Coupled with electronic structure calculations, the solute electronic structure can be used as a probe to generate a more detailed molecular understanding of the hydrogen bonding within solution by monitoring the ΔBE between the methyl and carbonyl carbons. In the presence of continuum solvation accounting for long-range electrostatic screening, the highly charged nature of the acetate conjugate base required more explicit solvent molecules (20 water molecules) when calculating the electronic structure of the solvation environment in order to reproduce the photoelectron experimental data. In comparison, acetic acid required only 1 water molecule in order to replicate the experimental photoelectron results. These findings are consistent with prior theoretical results on the solvation-dependence of ionization potentials,[44] including the observation that the accuracy of continuum solvation models deteriorates for charged species.[45]

Supplementary Information

XPS spectra, summary table of relevant values and calculated ΔBE of d^4-acetic acid in aqueous solution are given free of charge in the supporting information

Acknowledgments

The lab-based ambient pressure X-ray photoelectron spectrometer was developed with funding from the W. M. Keck Foundation. K.Z. would like to graciously thank the Beckman Scholar Program funded by the Arnold and Mabel Beckman Foundation. This material is based upon

work supported by the National Science Foundation under CHE-1800431 and

CHE-2102568.21025682102568

References

(1) Fuson, N.; Josien, M. Structure of the Associated OH Valence Vibration Band in Light and Heavy Acetic, Trichloroacetic, and Trifluoroacetic Acids. *J. Opt. Soc. Am.* **2008**, *43* (11), 1102.
(2) Lange, K. M.; Suljoti, E.; Aziz, E. F. Resonant Inelastic X-Ray Scattering as a Probe of Molecular Structure and Electron Dynamics in Solutions. *J. Electron Spectrosc. Relat. Phenom.* **2013**, *188*, 101–110.
(3) Reichardt, C. *Solvents and Solvent Effects in Organic Chemistry*.
(4) Asfin, R. E. IR Spectra of Hydrogen-Bonded Complexes of Trifluoroacetic Acid with Acetone and Diethyl Ether in the Gas Phase. Interaction between CH and OH Stretching Vibrations. *J. Phys. Chem. A* **2019**, *123* (15), 3285–3292.
(5) Max, J. J.; Chapados, C. Infrared Spectroscopy of Aqueous Carboxylic Acids: Comparison between Different Acids and Their Salts. *J. Phys. Chem. A* **2004**, *108* (16), 3324–3337.
(6) Ruderman, G.; Caffarena, E. R.; Mogilner, I. G.; Tolosa, E. J. Hydrogen Bonding of Carboxylic Acids in Aqueous Solutions - UV Spectroscopy, Viscosity, and Molecular Simulation of Acetic Acid. *J. Solut. Chem.* **1998**, *27* (10), 935–948.
(7) Sellberg, J. A.; McQueen, T. A.; Laksmono, H.; Schreck, S.; Beye, M.; Deponte, D. P.; Kennedy, B.; Nordlund, D.; Sierra, R. G.; Schlesinger, D.; et al. X-Ray Emission Spectroscopy of Bulk Liquid Water in No-Man's Land. *J. Chem. Phys.* **2015**, *142* (4).
(8) Lange, K. M.; Suljoti, E.; Aziz, E. F. Resonant Inelastic X-Ray Scattering as a Probe of Molecular Structure and Electron Dynamics in Solutions. *J. Electron Spectrosc. Relat. Phenom.* **2013**, *188*, 101–110.
(9) Vaz da Cruz, V.; Gel'mukhanov, F.; Eckert, S.; Iannuzzi, M.; Ertan, E.; Pietzsch, A.; Couto, R. C.; Niskanen, J.; Fondell, M.; Dantz, M.; Schmitt, T.; Lu, X.; McNally, D.; Jay, R. M.; Kimberg, V.; Föhlisch, A.; Odelius, M. Probing Hydrogen Bond Strength in Liquid Water by Resonant Inelastic X-Ray Scattering. *Nat. Commun.* **2019**, *10* (1), 1013.
(7) Voora, V. K.; Galhenage, R.; Hemminger, J. C.; Furche, F. Effective One-Particle Energies from Generalized Kohn–Sham Random Phase Approximation: A Direct Approach for Computing and Analyzing Core Ionization Energies. *J. Chem. Phys.* **2019**, *151* (13), 134106.
(11) Zhang, M.; Chen, L.; Yang, H.; Ma, J. Theoretical Study of Acetic Acid Association Based on Hydrogen Bonding Mechanism. *J. Phys. Chem. A* **2017**, *121* (23), 4560–4568.
(12) Nagy, P. I.; Smith, D. A.; Alagona, G.; Ghio, C. Ab Initio Studies of Free and Monohydrated Carboxylic Acids in the Gas Phase. *J. Phys. Chem.* **1994**, *98* (2), 486–493.
(13) Winter, B. Liquid Microjet for Photoelectron Spectroscopy. *Nucl. Instrum. Methods Phys. Res. Sect. Accel. Spectrometers Detect. Assoc. Equip.* **2009**, *601* (1–2), 139–150.
(14) Margarella, A. M.; Perrine, K. A.; Lewis, T.; Faubel, M.; Winter, B.; Hemminger, J. C. Dissociation of Sulfuric Acid in Aqueous Solution: Determination of the Photoelectron Spectral Fingerprints of H2SO4, HSO 4 -, and SO4 2- in Water. *J. Phys. Chem. C* **2013**, *117* (16), 8131–8137.

(15) Winter, B.; Faubel, M. Photoemission from Liquid Aqueous Solutions. *Chem. Rev.* **2006**, *106* (4), 1176–1211.
(16) Winter, B.; Weber, R.; Widdra, W.; Dittmar, M.; Faubel, M.; Hertel, I. V. Full Valence Band Photoemission from Liquid Water Using EUV Synchrotron Radiation. *J. Phys. Chem. A* **2004**, *108* (14), 2625–2632.
(17) Lewis, T.; Winter, B.; Stern, A. C.; Baer, M. D.; Mundy, C. J.; Tobias, D. J.; Hemminger, J. C. Dissociation of Strong Acid Revisited: X-Ray Photoelectron Spectroscopy and Molecular Dynamics Simulations of HNO3 in Water. *J. Phys. Chem. B* **2011**, *115* (30), 9445–9451.
(18) Lewis, T.; Faubel, M.; Winter, B.; Hemminger, J. C. CO2 Capture in Amine-Based Aqueous Solution: Role of the Gas-Solution Interface. *Angew. Chem. Int. Ed.* **2011**, *50* (43), 10178–10181.
(19) Ghosh, D.; Isayev, O.; Slipchenko, L. V.; Krylov, A. I. Effect of Solvation on the Vertical Ionization Energy of Thymine: From Microhydration to Bulk. *J. Phys. Chem. A* **2011**, *115* (23), 6028–6038.
(20) Löytynoja, T.; Niskanen, J.; Jänkälä, K.; Vahtras, O.; Rinkevicius, Z.; Ågren, H. Quantum Mechanics/Molecular Mechanics Modeling of Photoelectron Spectra: The Carbon 1s Core–Electron Binding Energies of Ethanol–Water Solutions. *J. Phys. Chem. B* **2014**, *118* (46), 13217–13225.
(21) Olivieri, G.; Parry, K. M.; Powell, C. J.; Tobias, D. J.; Brown, M. A. Quantitative Interpretation of Molecular Dynamics Simulations for X-Ray Photoelectron Spectroscopy of Aqueous Solutions. *J. Chem. Phys.* **2016**, *144* (15).
(22) Ghosal, S.; Hemminger, J. C.; Bluhm, H.; Mun, B. S.; Hebenstreit, E. L. D.; Ketteler, G.; Ogletree, D. F.; Requejo, F. G.; Salmeron, M. Electron Spectroscopy of Aqueous Solution Interfaces Reveals Surface Enhancement of Halides. *Science* **2005**, *307* (5709), 563–566.
(23) Perrine, K. A.; Parry, K. M.; Stern, A. C.; Van Spyk, M. H. C.; Makowski, M. J.; Freites, J. A.; Winter, B.; Tobias, D. J.; Hemminger, J. C. Specific Cation Effects at Aqueous Solution−vapor Interfaces: Surfactant-like Behavior of Li + Revealed by Experiments and Simulations. *Proc. Natl. Acad. Sci.* **2017**, 201707540.
(24) Brown, M. A.; D'Auria, R.; Kuo, I. F. W.; Krisch, M. J.; Starr, D. E.; Bluhm, H.; Tobias, D. J.; Hemminger, J. C. Ion Spatial Distributions at the Liquid-Vapor Interface of Aqueous Potassium Fluoride Solutions. *Phys. Chem. Chem. Phys.* **2008**, *10* (32), 4778–4784.
(25) Makowski, M. J.; Stern, A. C.; Hemminger, J. C.; Tobias, D. J. Orientation and Structure of Acetonitrile in Water at the Liquid-Vapor Interface: A Molecular Dynamics Simulation Study. *J. Phys. Chem. C* **2016**, *120* (31), 17555–17563.
(26) Bruce, J. P.; Hemminger, J. C. Characterization of Fe^{2+} Aqueous Solutions with Liquid Jet X-Ray Photoelectron Spectroscopy: Chloride Depletion at the Liquid/Vapor Interface Due to Complexation with Fe^{2+}. *J. Phys. Chem. B* **2019**, *123* (39), 8285–8290.
(27) Makowski, M. J.; Galhenage, R. P.; Langford, J.; Hemminger, J. C. Liquid-Jet X-Ray Photoelectron Spectra of TiO2 Nanoparticles in an Aqueous Electrolyte Solution. *J. Phys. Chem. Lett.* **2016**, *7* (9), 1732–1735.
(28) Perdew, J. P.; Burke, K.; Ernzerhof, M. Generalized Gradient Approximation Made Simple. *Phys. Rev. Lett.* **1996**, *77* (18), 3865–3868.
(29) Weigend, F.; Häser, M.; Patzelt, H.; Ahlrichs, R. RI-MP2: Optimized Auxiliary Basis Sets and Demonstration of Efficiency. *Chem. Phys. Lett.* **1998**, *294* (1–3), 143–152.

(30) Weigend, F.; Ahlrichs, R. Balanced Basis Sets of Split Valence, Triple Zeta Valence and Quadruple Zeta Valence Quality for H to Rn: Design and Assessment of Accuracy. *Phys. Chem. Chem. Phys.* **2005**, *7* (18), 3297.
(31) Schäfer, A.; Klamt, A.; Sattel, D.; Lohrenz, J. C. W.; Eckert, F. COSMO Implementation in TURBOMOLE: Extension of an Efficient Quantum Chemical Code towards Liquid Systems. *Phys. Chem. Chem. Phys.* **2000**, *2* (10), 2187–2193.
(32) Klamt, A.; Schüürmann, G. COSMO: A New Approach to Dielectric Screening in Solvents with Explicit Expressions for the Screening Energy and Its Gradient. *J Chem Soc Perkin Trans 2* **1993**, No. 5, 799–805.
(33) Haynes, W. M. *CRC Handbook of Chemistry and Physics*, 93rd ed.; CRC Press: Boca Raton, FL, 2012.
(34) Tse, J. S. Ab Initio Molecular Dynamics with Density Functional Theory. *Annu. Rev. Phys. Chem.* **2002**, *53* (1), 249–290.
(35) Avogadro: An Advanced Semantic Chemical Editor https://www.ncbi.nlm.nih.gov/pmc/articles/PMC3542060/ (accessed 2020 -06 -13).
(36) Balasubramani, S. G.; Chen, G. P.; Coriani, S.; Diedenhofen, M.; Frank, M. S.; Franzke, Y. J.; Furche, F.; Grotjahn, R.; Harding, M. E.; Hättig, C.; et al. TURBOMOLE: Modular Program Suite for *Ab Initio* Quantum-Chemical and Condensed-Matter Simulations. *J. Chem. Phys.* **2020**, *152* (18), 184107.
(37) Bryantsev, V. S.; Diallo, M. S.; van Duin, A. C. T.; Goddard III, W. A. Hydration of Copper(II): New Insights from Density Functional Theory and the COSMO Solvation Model. *J. Phys. Chem. A* **2008**, *112* (38), 9104–9112.
(38) Fairley, N.; Carrick, A. *The Casa Cookbook*; 2005.
(39) Chocholoušová, J.; Vacek, J.; Hobza, P. Acetic Acid Dimer in the Gas Phase, Nonpolar Solvent, Microhydrated Environment, and Dilute and Concentrated Acetic Acid: Ab Initio Quantum Chemical and Molecular Dynamics Simulations. *J. Phys. Chem. A* **2003**, *107* (17), 3086–3092.
(40) Krishnakumar, P.; Maity, D. K. Microhydration of Neutral and Charged Acetic Acid. *J. Phys. Chem. A* **2017**, *121* (2), 493–504.
(41) Fedotova, M. V.; Kruchinin, S. E. Hydration of Acetic Acid and Acetate Ion in Water Studied by 1D-RISM Theory. *J. Mol. Liq.* **2011**, *164* (3), 201–206.
(42) Barnett, R. N.; Landman, U.; Cleveland, C. L.; Jortner, J. Size Dependence of the Energetics of Electron Attachment to Large Water Clusters. *Chem. Phys. Lett.* **1988**, *145* (5), 382–386.
(43) Pathak, A. K.; Samanta, A. K.; Maity, D. K.; Mukherjee, T.; Ghosh, S. K. Generalized Microscopic Theory for the Detachment Energy of Solvated Negatively Charged Ions in Finite Size Clusters: A Step toward Bulk. *J. Phys. Chem. Lett.* **2010**, *1* (5), 886–890.
(44) Medina-Llanos, C.; Ågren, H.; Mikkelsen, K. V.; Jensen, H. J. Aa. Self-consistent Reaction Field Calculations of Photoelectron Binding Energies for Solvated Molecules. *J. Chem. Phys.* **1989**, *90* (11), 6422–6435.
(45) Dupont, C.; Andreussi, O.; Marzari, N. Self-Consistent Continuum Solvation (SCCS): The Case of Charged Systems. *J. Chem. Phys.* **2013**, *139* (21), 214110.

TOC Figure:

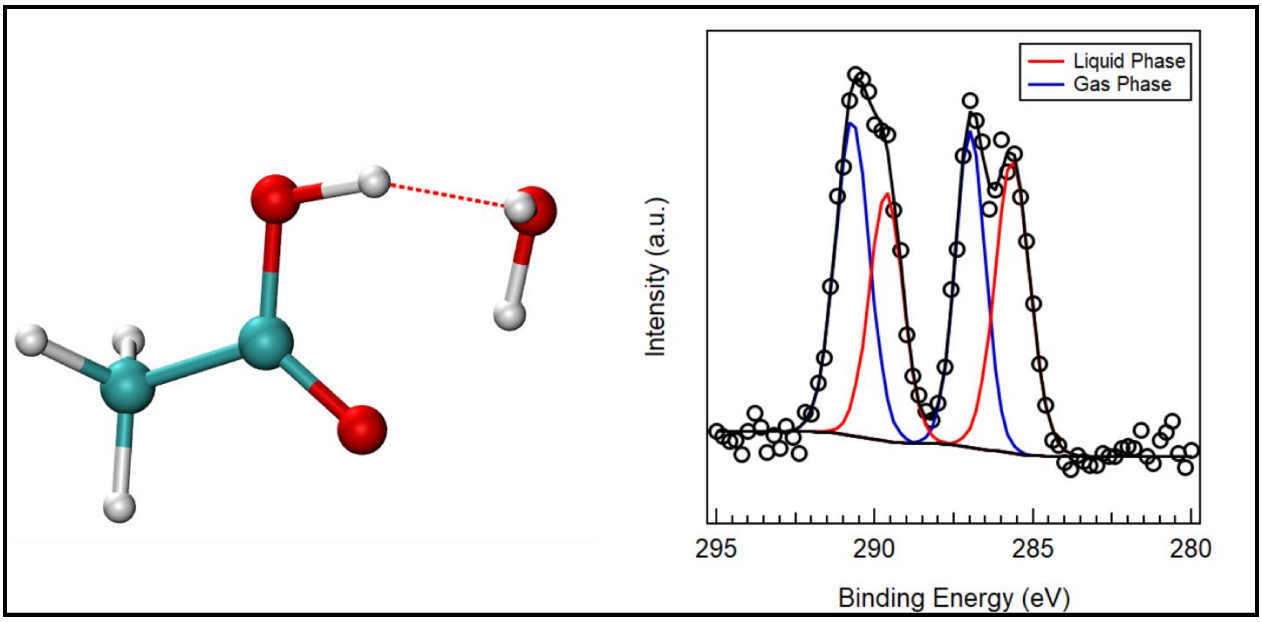
Liquid Phase
Gas Phase
Intensity (a.u.)
295
290
285
280
Binding Energy (eV)